



Contents lists available at ScienceDirect

Physics Letters B

www.elsevier.com/locate/physletb



Low-energy pion–pion scattering in the $pp \rightarrow pp\pi^+\pi^-$ and $p\bar{p} \rightarrow p\bar{p}\pi^+\pi^-$ reactions

P. Lebiedowicz^a, A. Szczurek^{a,b,*}, R. Kamiński^a

^a Institute of Nuclear Physics PAN, PL-31-342 Cracow, Poland

^b University of Rzeszów, PL-35-959 Rzeszów, Poland

ARTICLE INFO

Article history:

Received 30 April 2009

Received in revised form 10 September 2009

Accepted 10 September 2009

Available online 18 September 2009

Editor: A. Ringwald

PACS:

13.75.Cs

13.75.Lb

11.80.Et

ABSTRACT

We evaluate the contribution of pion–pion rescattering to the $pp \rightarrow pp\pi^+\pi^-$ and $p\bar{p} \rightarrow p\bar{p}\pi^+\pi^-$ reactions. We compare our results with the close-to-threshold experimental data. The pion–pion rescattering contribution is found there to be negligible. The predictions for future experiments with PANDA detector at High Energy Storage Ring (HESR) in GSI Darmstadt are presented. It is discussed how to cut off the dominant Roper resonance and double- Δ excitation mechanisms leading to the $pp\pi^+\pi^-$ channel in final state. Differential distributions in momentum transfers, transverse momentum, effective two-pions mass, relative azimuthal angle between pions, and pion rapidities are presented.

© 2009 Elsevier B.V. Open access under CC BY license.

1. Introduction

The $pp \rightarrow pp\pi^+\pi^-$ reaction, which is one of the reactions with four charged particles in the final state, can be easily measured. Very close to the threshold the excitation of the Roper resonance and its subsequent decay as well as double- Δ excitation constitute the dominant reaction mechanism [1]. Only energy dependence of the total cross section was discussed in [1]. The pion–pion rescattering mechanism shown in Fig. 1 was not discussed so far in the literature.¹

On the other hand a significant progress in studying pion–pion scattering at low-energy has been recently achieved due to works based on dispersive analyses of experimental data [3–8]. These works, led to precise determination of the $\pi\pi$ scattering amplitudes consistent with analyticity, unitarity, crossing symmetry and chiral perturbation theory (χ PT) within error bars. Strong theoretical constraints from forward dispersion relations and sum rules allowed to test several, sometimes conflicting sets of data [7]. The twice subtracted dispersion relations (Roy's equations) used in

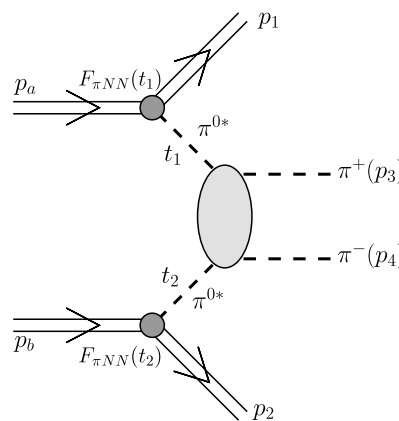


Fig. 1. The pion–pion rescattering mechanisms of exclusive production of π^+ and π^- in proton–proton and proton–antiproton collisions. Some kinematical variables are shown explicitly. The stars attached to π^0 mesons denote the fact that they are off-mass-shell.

* Corresponding author at: Institute of Nuclear Physics PAN, PL-31-342 Cracow, Poland.

E-mail addresses: piotr.lebiedowicz@ifj.edu.pl (P. Lebiedowicz),

antoni.szczurek@ifj.edu.pl (A. Szczurek), robert.kaminski@ifj.edu.pl (R. Kamiński).

¹ The π^0 is an unstable particle with life time of the order 10^{-17} seconds [2]. This is orders of magnitude more than a typical strong interaction times. Therefore one can safely neglect the fact of the π^0 decay.

[3,4] allowed to calculate very precisely sigma pole position and S-wave scattering lengths a_0 and a_2 . These works were continued in Refs. [5–9]. In Ref. [6] the sigma position was determined from first principles with unprecedented precision. Recent works on once subtracted dispersion relations give results with similar precision [9]. Application of Roy's equations in another dispersive analysis of experimental data allowed to eliminate the long stand-

ing “up–down” ambiguity below 1 GeV in $l = S_0^2$ wave [10]. The simple and model independent amplitudes of the S_0 , P , S_2 , D_0 , D_2 , F and G waves presented in series of works [7–9] seem to be efficient and easy to use in analyses of $\pi\pi$ interactions. Amplitudes presented in [8] have been applied in this analysis to parameterize the final state interactions $\pi^0\pi^0 \rightarrow \pi^+\pi^-$.

The knowledge from the $\pi\pi \rightarrow \pi\pi$ reaction can almost directly be used in our $pp \rightarrow pp\pi\pi$ reaction shown in Fig. 1. It is the aim of this Letter to evaluate the pion–pion rescattering contribution for the measured close-to-threshold region of the $pp \rightarrow pp\pi^+\pi^-$ reaction as well as to make predictions for the future experiments with the PANDA detector at High Energy Storage Ring (HESR) in GSI Darmstadt for the $p\bar{p} \rightarrow p\bar{p}\pi^+\pi^-$ reaction.

2. The two-pion rescattering amplitude

It is straightforward to evaluate the pion–pion exchange current contribution shown in Fig. 1. If we assume the $i\gamma_5$ type coupling of the pion to the nucleon then the Born amplitude squared and averaged over initial and summed over final spin polarizations reads:

$$\begin{aligned} |\overline{\mathcal{M}}|^2 = & \frac{1}{4} \left[(E_a + m)(E_1 + m) \left(\frac{\mathbf{p}_a^2}{(E_a + m)^2} + \frac{\mathbf{p}_1^2}{(E_1 + m)^2} \right. \right. \\ & \left. \left. - \frac{2\mathbf{p}_a \cdot \mathbf{p}_1}{(E_a + m)(E_1 + m)} \right) \right] \times 2 \frac{g_{\pi NN}^2}{(t_1 - m_\pi^2)^2} F_{\pi NN}^2(t_1) \\ & \times |\mathcal{M}_{\pi^0\pi^0 \rightarrow \pi^+\pi^-}(s_{34}, \cos\theta^*, t_1, t_2)|^2 \\ & \times \frac{g_{\pi NN}^2}{(t_2 - m_\pi^2)^2} F_{\pi NN}^2(t_2) \\ & \times \left[(E_b + m)(E_2 + m) \left(\frac{\mathbf{p}_b^2}{(E_b + m)^2} + \frac{\mathbf{p}_2^2}{(E_2 + m)^2} \right. \right. \\ & \left. \left. - \frac{2\mathbf{p}_b \cdot \mathbf{p}_2}{(E_b + m)(E_2 + m)} \right) \right] \times 2. \end{aligned} \quad (2.1)$$

In the formula above m is the mass of the nucleon, E_a , E_b and E_1 , E_2 are the energies of initial and outgoing nucleons, \mathbf{p}_a , \mathbf{p}_b and \mathbf{p}_1 , \mathbf{p}_2 are the corresponding three-momenta and m_π is the pion mass. The factor $g_{\pi NN}$ is the familiar pion–nucleon coupling constant and is relatively well known [11] ($\frac{g_{\pi NN}^2}{4\pi} = 13.5\text{--}14.6$).

In the case of central production of pion pairs not far from the threshold region rather large transferred four-momenta squared t_1 and t_2 are involved and one has to include non-point-like and off-shellness nature of the particles involved in corresponding vertices. This is incorporated via the $F_{\pi NN}(t_1)$ or $F_{\pi NN}(t_2)$ vertex form factors. We shall discuss how the uncertainties of the form factors influence our final results. In the meson exchange approach [12] they are parameterized in the monopole form as

$$F_{\pi NN}(t_{1,2}) = \frac{\Lambda^2 - m_\pi^2}{\Lambda^2 - t_{1,2}}. \quad (2.2)$$

In the following for brevity we shall use notation $t_{1,2}$ which means t_1 or t_2 . Typical values of the form factor parameters are $\Lambda = 1.2\text{--}1.4$ GeV [12], however the Gottfried Sum Rule violation prefers smaller $\Lambda \approx 0.8$ GeV [13].

The amplitude of the subprocess $\pi^0\pi^0 \rightarrow \pi^+\pi^-$ with virtual initial pions is written in terms of the amplitude for real initial pions and correction factors as:

$$\begin{aligned} \mathcal{M}_{\pi^0\pi^0 \rightarrow \pi^+\pi^-}(s_{34}, \cos\theta^*, t_1, t_2) \\ = \mathcal{M}_{\pi^0\pi^0 \rightarrow \pi^+\pi^-}(s_{34}, \cos\theta^*) F_{\pi^0}(t_1) F_{\pi^0}(t_2). \end{aligned} \quad (2.3)$$

The on-shell amplitude can be expanded into partial wave amplitudes $f_l^I(s_{34})$ with angular momentum l and isospin I :

$$\mathcal{M}(s_{34}, \cos\theta^*) = 16\pi \sum_I \sum_l (2l+1) P_l(\cos\theta^*) f_l^I(s_{34}). \quad (2.4)$$

For a limited range of $M_{\pi\pi} = \sqrt{s_{34}}$ it is enough to take only a few partial waves. In our calculation $f_l^I(s_{34})$ can be parameterized in terms of the pion–pion phase shifts $\delta_l^I(s_{34})$ and the inelasticities $\eta_l^I(s_{34})$ taken from [8]

$$f_l^I(s_{34}) = \sqrt{\frac{s_{34}}{s_{34} - 4m_\pi^2}} \frac{\eta_l^I(s_{34}) e^{2i\delta_l^I(s_{34})} - 1}{2i}. \quad (2.5)$$

In the formula above $F_{\pi^0}(t_{1,2})$ are extra correction factors due to off-shellness of initial pions. We use exponential form factors of the type

$$F_{\pi^0}(t_{1,2}) = \exp\left(\frac{t_{1,2} - m_\pi^2}{\Lambda_{\text{off}}^2}\right), \quad (2.6)$$

i.e. normalized to unity on the pion-mass-shell. In general, the parameter Λ_{off} is not known but in principle could be fitted to the experimental data providing that our mechanism is the dominant mechanism which can be true only in a limited corner of the phase space. From our general experience in hadronic physics we expect $\Lambda_{\text{off}} \sim 1$ GeV.

The $\cos\theta^*$ in Eq. (2.4) requires a separate discussion. In the on-shell case the $\cos\theta$ can be expressed in terms of the two-body Mandelstam invariants \hat{t} and \hat{u} in two equivalent ways:

$$\begin{aligned} \cos\theta_{\hat{t}} &= 1 + \frac{2\hat{t}}{s_{34} - 4m_\pi^2}, \\ \cos\theta_{\hat{u}} &= -1 - \frac{2\hat{u}}{s_{34} - 4m_\pi^2}. \end{aligned} \quad (2.7)$$

This can be generalized to the case of off-shell initial pions as:

$$\begin{aligned} \cos\theta_{\hat{t}}^* &= 1 + \frac{2\hat{t}}{s_{34} - m_\pi^2 - m_\pi^2 - t_1 - t_2}, \\ \cos\theta_{\hat{u}}^* &= -1 - \frac{2\hat{u}}{s_{34} - m_\pi^2 - m_\pi^2 - t_1 - t_2}. \end{aligned} \quad (2.8)$$

In our case of the $2 \rightarrow 4$ reaction³ we have to deal with off-shell initial pions and an analytical continuation of formula (2.8) is required. In the following we use the most straightforward prescription:

$$\cos\theta^* = \frac{1}{2} (\cos\theta_{\hat{t}}^* + \cos\theta_{\hat{u}}^*) = \frac{\hat{t} - \hat{u}}{s_{34} - m_\pi^2 - m_\pi^2 - t_1 - t_2}. \quad (2.9)$$

The formula above reproduces the on-shell formula (2.7) when $t_1 \rightarrow m_\pi^2$ and $t_2 \rightarrow m_\pi^2$, is symmetric with respect to \hat{t} and \hat{u} and fulfils the requirement $-1 < \cos\theta^* < 1$.

The differential cross sections for the $2 \rightarrow 4$ reaction are calculated using the general formula

$$\begin{aligned} d\sigma = & \frac{1}{2s} |\overline{\mathcal{M}}|^2 (2\pi)^4 \delta^4(p_a + p_b - p_1 - p_2 - p_3 - p_4) \\ & \times \frac{d^3p_1}{(2\pi)^3 2E_1} \frac{d^3p_2}{(2\pi)^3 2E_2} \frac{d^3p_3}{(2\pi)^3 2E_3} \frac{d^3p_4}{(2\pi)^3 2E_4}. \end{aligned} \quad (2.10)$$

² Here l is angular momentum between pions and I is the total isospin of the pion pair.

³ $2 \rightarrow 4$ reaction denotes a type of the reaction with two initial and four final particles.

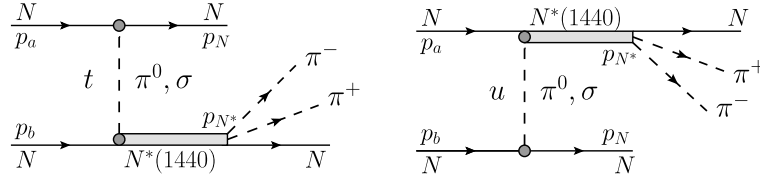


Fig. 2. The dominant mechanisms of Roper resonance production at low energy proton–proton scattering.

3. Reactions via Roper resonance excitation and its decay

Close to the two-pions production threshold the dominant mechanism for the reaction $pp \rightarrow pp\pi^+\pi^-$ is Roper resonance excitation and its subsequent three-body decay [1,14]. This mechanism constitutes an “unwanted background” to our pion–pion rescattering. At low energy the sigma and pion exchanges are the dominant mechanisms of Roper resonance excitation (see [15]). Here we show how to approximately estimate the phase-space integrated contribution of the mechanism shown in Fig. 2 not very close to the threshold.⁴

The amplitude for the Roper resonance N^* excitation via σ -meson exchange can be written as

$$\begin{aligned} \mathcal{M}_{\lambda_a \lambda_b \rightarrow \lambda_N \lambda_{N^*}}^{(\sigma, t)} &= g_{\sigma NN} F_{\sigma NN}(t) [\bar{u}(p_N, \lambda_N) u(p_a, \lambda_a)] \frac{1}{t - m_\sigma^2} \\ &\quad \times g_{\sigma NN^*} F_{\sigma NN^*}(t) [\bar{u}(p_{N^*}, \lambda_{N^*}) u(p_b, \lambda_b)], \\ \mathcal{M}_{\lambda_a \lambda_b \rightarrow \lambda_N \lambda_{N^*}}^{(\sigma, u)} &= g_{\sigma NN^*} F_{\sigma NN^*}(u) [\bar{u}(p_{N^*}, \lambda_{N^*}) u(p_a, \lambda_a)] \frac{1}{u - m_\sigma^2} \\ &\quad \times g_{\sigma NN} F_{\sigma NN}(u) [\bar{u}(p_N, \lambda_N) u(p_b, \lambda_b)]. \end{aligned} \quad (3.1)$$

The amplitude for the Roper resonance excitation via π -exchange mechanism can be written as

$$\begin{aligned} \mathcal{M}_{\lambda_a \lambda_b \rightarrow \lambda_N \lambda_{N^*}}^{(\pi, t)} &= g_{\pi NN} F_{\pi NN}(t) [\bar{u}(p_N, \lambda_N) i\gamma_5 u(p_a, \lambda_a)] \frac{1}{t - m_\pi^2} \\ &\quad \times g_{\pi NN^*} F_{\pi NN^*}(t) [\bar{u}(p_{N^*}, \lambda_{N^*}) i\gamma_5 u(p_b, \lambda_b)], \\ \mathcal{M}_{\lambda_a \lambda_b \rightarrow \lambda_N \lambda_{N^*}}^{(\pi, u)} &= g_{\pi NN^*} F_{\pi NN^*}(u) [\bar{u}(p_{N^*}, \lambda_{N^*}) i\gamma_5 u(p_a, \lambda_a)] \frac{1}{u - m_\pi^2} \\ &\quad \times g_{\pi NN} F_{\pi NN}(u) [\bar{u}(p_N, \lambda_N) i\gamma_5 u(p_b, \lambda_b)]. \end{aligned} \quad (3.2)$$

In the above equations $g_{\pi NN}$, $g_{\sigma NN}$, $g_{\pi NN^*}$, $g_{\sigma NN^*}$ represent the coupling constants and N denotes proton or antiproton; $u(p_a, \lambda_a)$, $u(p_b, \lambda_b)$, $u(p_N, \lambda_N)$, $u(p_{N^*}, \lambda_{N^*})$ are the spinors of the protons and Roper resonance; p_N and p_{N^*} denote the four-momenta of the outgoing proton and the Roper resonance; λ_N and λ_{N^*} the helicities of the nucleon and the Roper resonance; t and u are the four-momentum transfers; m_π and m_σ are the mass of the pion and sigma mesons.

In our calculations the coupling constants are taken as $g_{\pi NN}^2/4\pi = 13.6$ [11], $g_{\sigma NN}^2/4\pi = 5.69$ [12], $g_{\pi NN^*}^2/4\pi = 2.0$ and $g_{\sigma NN^*}^2/4\pi = 2.0$. Because numerically the σ -exchange is the dominant mechanism and the π -exchange is only a small correction,⁵ in practice the latter can be neglected. The coupling constant $g_{\sigma NN^*}$

is in fact an unknown parameter which in principle should be determined from the experimental data. Different values have been used in the literature [12,16]. Our number is an average value of those found in the literature. We parameterize the form factors $F_{\sigma NN}(t, u)$ (and $F_{\pi NN}(t, u)$) either in the monopole form with cut-off parameter Λ_M as traditionally for low energy processes:

$$F_{\sigma NN}(t, u) = \frac{\Lambda_M^2 - m_\sigma^2}{\Lambda_M^2 - t, u}, \quad (3.3)$$

or in the exponential form often used at high energies with cut-off parameter Λ_E :

$$F_{\sigma NN}(t, u) = \exp\left(\frac{t, u - m_\sigma^2}{\Lambda_E^2}\right). \quad (3.4)$$

The angular distribution for single Roper resonance excitation can be calculated from the amplitude above as

$$\begin{aligned} \frac{d\sigma_{pp \rightarrow pN^*(1440)}}{d\Omega} &= \frac{1}{64\pi^2 s} \left(\frac{q_f}{q_i}\right) \frac{1}{4} \\ &\quad \times \sum_{\lambda_a \lambda_b \lambda_N \lambda_{N^*}} |\mathcal{M}_{\lambda_a \lambda_b \rightarrow \lambda_N \lambda_{N^*}}^{(t)}(z) - \mathcal{M}_{\lambda_a \lambda_b \rightarrow \lambda_N \lambda_{N^*}}^{(u)}(z)|^2, \end{aligned} \quad (3.5)$$

where s is a square of the proton–proton center-of-mass energy; q_i and q_f are center-of-mass momenta in the initial pp or the final pN^* systems, respectively and $z = \cos\theta$, where θ is the center-of-mass angle between the outgoing and initial nucleon. The factor $\frac{1}{4}$ and $\sum_{\lambda_a \lambda_b \lambda_N \lambda_{N^*}}$ emerge for the simple reason that the polarization of initial and final particles is not considered. In general, one should calculate the cross section for $2 \rightarrow 4$ reaction based on diagrams shown in Fig. 2 with Roper resonance in the intermediate state (in general off-shell particle). However, for sufficiently high energies the total cross section for the $pp\pi^+\pi^-$ final state can be written approximately as a cross section for the Roper resonance excitation and a probability for the $N^*(1440) \rightarrow p\pi^+\pi^-$ decay (on-shell approximation):

$$\begin{aligned} \sigma_{pp \rightarrow pp\pi^+\pi^-}(\sqrt{s}) &\approx \sigma_{pp \rightarrow pN^*(1440)}(\sqrt{s}) \cdot \text{Br}(N^*(1440) \rightarrow p\pi^+\pi^-). \end{aligned} \quad (3.6)$$

This formula will be used to calculate the total cross section for the Roper resonance mechanism to show as a reference for the discussed above two-pion rescattering contribution. The branching ratio to the $p\pi^+\pi^-$ channel is not very well known and the mechanism of the Roper resonance decay can be complicated. Particle Data Book contains only branching fraction for all $N\pi\pi$ states. Our decay channel ($p\pi^+\pi^-$) is only one out of three possible ($p\pi^0\pi^0$, $p\pi^+\pi^-$, $n\pi^+\pi^0$). We take $\text{Br}(N^*(1440) \rightarrow p\pi^+\pi^-) = 0.1$.

In principle, all processes (pion rescattering, Roper production and decay, etc.) add coherently and can interfere. At low energy, where the phase space is very limited the interference seems unavoidable. Some distance from the threshold (of our main interest) they may occupy different regions of the phase space. This automatically means small interference effects. In our preliminary

⁴ Very close to the threshold the reaction must be treated as genuine four-body reaction with the $pp\pi^+\pi^-$ final state (see [1]).

⁵ The difference is due to scalar coupling for σ -exchange or pseudoscalar γ_5 coupling for pion exchange.

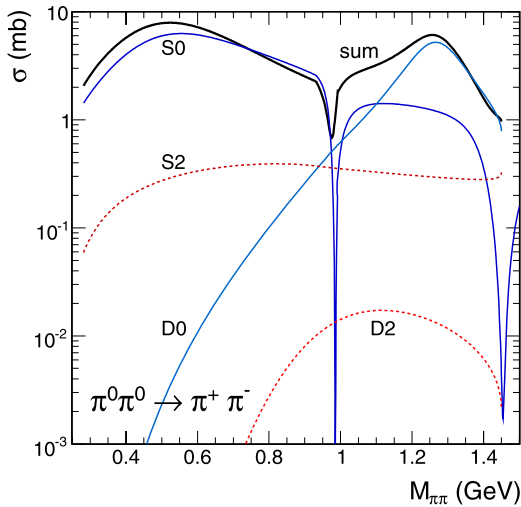


Fig. 3. The angle-integrated cross section for the reaction $\pi^0\pi^0 \rightarrow \pi^+\pi^-$. The thick solid line represents the coherent sum of all partial waves. The contributions for individual partial waves S_0 , S_2 , D_0 and D_2 are shown for comparison.

calculation we have estimated the Roper resonance contribution in a simplified way (in terms of the two-body reaction amplitude and a probability of the 3-body decay). In order to address numerically the interference effects with pion rescattering the Roper resonance must be treated as a genuine four-body processes. This requires a modelling of the 3-body Roper resonance decay (not necessarily simple as different sequential processes are possible). To avoid the rather complicated problem of the interference we proposed instead imposing extra kinematical cuts which is possible at sufficiently large energies.

In the next section we shall show our predictions for several differential distributions in different variables.

4. Results

Before we go to our four-body reaction let us stay for a moment with the $\pi^0\pi^0 \rightarrow \pi^+\pi^-$ on-shell scattering. In Fig. 3 we show the total (angle-integrated) cross section for the $\pi^0\pi^0 \rightarrow \pi^+\pi^-$ process which constitutes the subprocess in the $2 \rightarrow 4$ reactions discussed in the present Letter. Here the partial wave expansion (2.4) with δ_l^i and η_l^i parameterizations from Ref. [8] were used. In the present work we have limited to $M_{\pi\pi} < 1.5$ GeV, i.e. energies relevant for WASA and future PANDA experiments.

At higher \sqrt{s} larger $M_{\pi\pi}$ energies may contribute. This will be discussed elsewhere [17]. We show also individual contributions of different partial waves: $(l, I) = (0, 0)$, $(0, 2)$, $(2, 0)$ and $(2, 2)$. Because of identity of particles in the initial state only partial waves with even l contribute. One can see characteristic bumps related to the famous scalar-isoscalar σ -meson at $M_{\pi\pi} \approx 0.5$ – 0.6 GeV and the tensor-isoscalar $f_2(1270)$. The dip at $M_{\pi\pi} = 980$ MeV is due to interference of the σ with another scalar-isoscalar narrow $f_0(980)$ meson. Generally the contributions of nonresonant partial waves with $l = 2$ are much smaller than those for $l = 0$.

In Fig. 4 we show the proton energy excitation function of the integral cross section for the $pp \rightarrow pp\pi^+\pi^-$ reaction. In addition, we compare our results with the experimental data for the $pp \rightarrow pp\pi^+\pi^-$ reaction (from Refs. [18–26]) and for the $p\bar{p} \rightarrow p\bar{p}\pi^+\pi^-$ one (only data from the JETSET (PS202) experiment at LEAR [27]). We present previous data (open symbols) with low statistics coming mainly from bubble-chamber measurements on hydrogen or on deuterium from Refs. [18–21] as well as one datum point from an inclusive spectrometer measurement at 800 MeV [22]. The newer

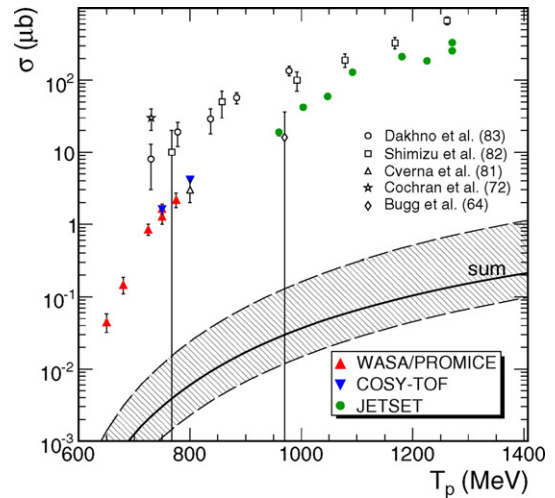


Fig. 4. The phase-space integrated cross section for the $pp \rightarrow pp\pi^+\pi^-$ reaction as a function of the proton kinetic energy in the laboratory frame T_p together with the experimental data from Refs. [18–27]. The thick solid line is explained in the text. The uncertainties band is also shown. In all cases a coherent sum of all partial waves is taken.

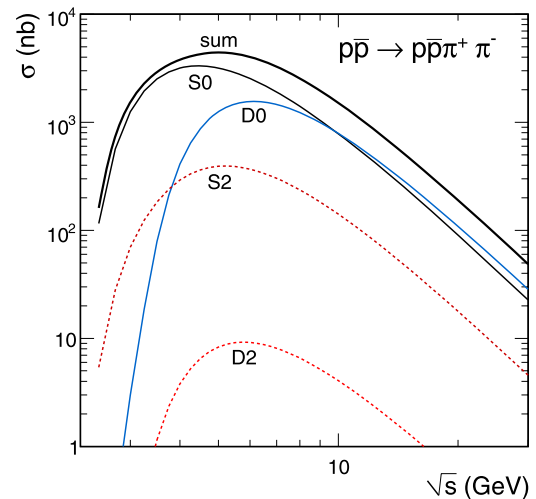


Fig. 5. The phase-space integrated cross section for the reaction $p\bar{p} \rightarrow p\bar{p}\pi^+\pi^-$ as a function of center of mass energy \sqrt{s} . The thick solid line represents the coherent sum of all partial waves. The contributions for individual partial waves S_0 , S_2 , D_0 and D_2 are shown for comparison.

data taken from Refs. [23–27] (full symbols) are much closer to the threshold of the reaction and are an order of magnitude smaller. We show how the uncertainties of the form factor parameters Λ affect our final results. For the pion-pion rescattering we modify the cut-off parameter Λ in Eq. (2.2) ($\Lambda \in (0.8, 1.4)$ GeV) and the cut-off parameter Λ_{off} in Eq. (2.6) ($\Lambda_{\text{off}} \in (0.5, 2.0)$ GeV). The thick solid line show theoretical predictions from the model calculations with $\Lambda = 0.8$ GeV and $\Lambda_{\text{off}} = 1.0$ GeV. The pion-pion rescattering contribution is found to be negligible.

As discussed in the theory section, the $\pi^0\pi^0 \rightarrow \pi^+\pi^-$ amplitude used for the $\pi^0\pi^0 \rightarrow \pi^+\pi^-$ reaction can, after a small “correction” for virtualities of both initial π^0 's, be used for the four-body process of our main interest. In Fig. 5 we show the total cross section (integrated over the whole phase space with the restriction $M_{\pi\pi} < 1.42$ GeV) for the four-body reaction as a function of the overall center-of-mass energy \sqrt{s} . We show the coherent sum of partial waves for different l and I as well as individual contributions. The maximum of the cross section occurs

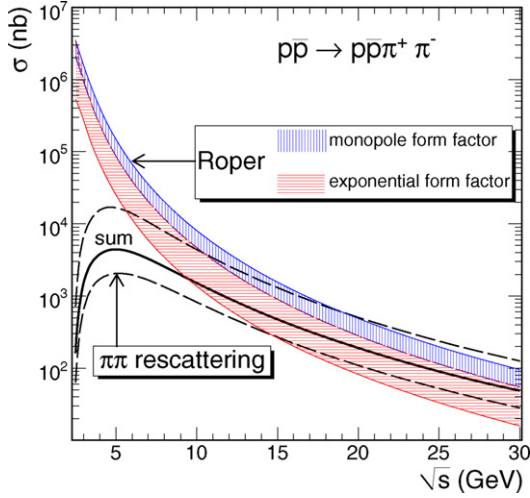


Fig. 6. The phase-space integrated cross section for the reaction $p\bar{p} \rightarrow p\bar{p}\pi^+\pi^-$ as a function of center of mass energy \sqrt{s} . We compare the pion-pion rescattering contribution and the Roper resonance contribution (only σ -meson exchange included). The uncertainty bands for both contributions are also shown. The area of uncertainties for the pion-pion rescattering contribution is indicated by the dashed lines. The pion-pion rescattering contribution is a coherent sum of all partial waves.

at $\sqrt{s} \approx 5$ GeV, i.e. at the highest energy planned for the FAIR HESR. The $l=0, l=0$ partial wave has the dominant contribution. The sum of the individual contributions is not equal to the cross section calculated with the sum of the partial wave amplitudes because of relatively strong interference effects.

In Fig. 6 we compare the pion-pion rescattering contribution and the contribution of Roper resonance excitation through σ -meson exchange. In both cases we have estimated the uncertainties of the contributions. For the pion-pion rescattering we modify Λ in Eq. (2.2) ($\Lambda \in (0.8, 1.4)$ GeV) and Λ_{off} in Eq. (2.6) ($\Lambda_{\text{off}} \in (0.5, 2.0)$ GeV). The bottom dashed line was obtained with $\Lambda = 0.8$ GeV and $\Lambda_{\text{off}} = 0.5$ GeV while the top dashed line with $\Lambda = 1.4$ GeV and $\Lambda_{\text{off}} = 2.0$ GeV. For the contribution of the Roper resonance excitation through σ -meson exchange we modify $\Lambda_M \in (1.5, 2.0)$ GeV (band with vertical lines) in the monopole parameterization and $\Lambda_E \in (1.0, 1.5)$ GeV (band with horizontal lines) in the exponential parameterization.

Because at low energies the Roper resonance excitation and double- Δ excitation play the dominant role it is not obvious how to extract the pion-pion rescattering contributions. To cut off the Roper resonance excitation contribution we eliminate from the phase space those cases when:

$$(M_{N^*} - \Delta M_{N^*} < M_{134} < M_{N^*} + \Delta M_{N^*})$$

or

$$(M_{N^*} - \Delta M_{N^*} < M_{234} < M_{N^*} + \Delta M_{N^*}).$$

To suppress the double- Δ excitation we eliminate from the phase space those cases when:

$$(M_{\Delta} - \Delta M_{\Delta} < M_{13} < M_{\Delta} + \Delta M_{\Delta} \quad \text{and}$$

$$M_{\Delta} - \Delta M_{\Delta} < M_{24} < M_{\Delta} + \Delta M_{\Delta})$$

or

$$(M_{\Delta} - \Delta M_{\Delta} < M_{14} < M_{\Delta} + \Delta M_{\Delta} \quad \text{and}$$

$$M_{\Delta} - \Delta M_{\Delta} < M_{23} < M_{\Delta} + \Delta M_{\Delta}).$$

Above M_{ijk} and M_{ik} represent effective mass of the $p\pi\pi$ and $p\pi$ systems, respectively; ΔM_{N^*} and ΔM_{Δ} are cut-off parameters. We

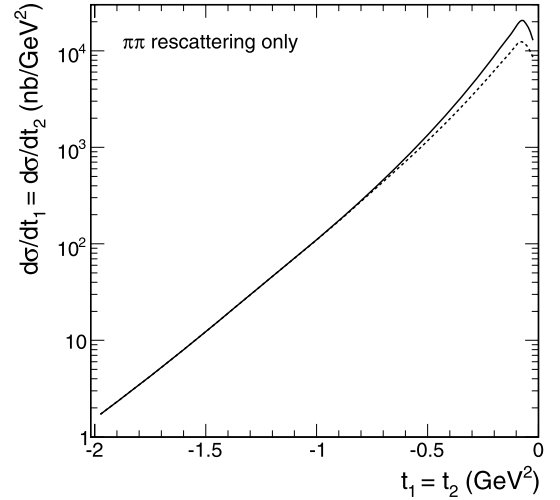


Fig. 7. Differential cross section $\frac{d^2\sigma}{dt_1 dt_2} = \frac{d\sigma}{dt_1} = \frac{d\sigma}{dt_2}$ for the $p\bar{p} \rightarrow p\bar{p}\pi^+\pi^-$ reaction at $\sqrt{s} = 5.5$ GeV. The solid line is the cross section without cuts, the dashed line includes cuts to remove regions of Roper resonance and double- Δ excitations.

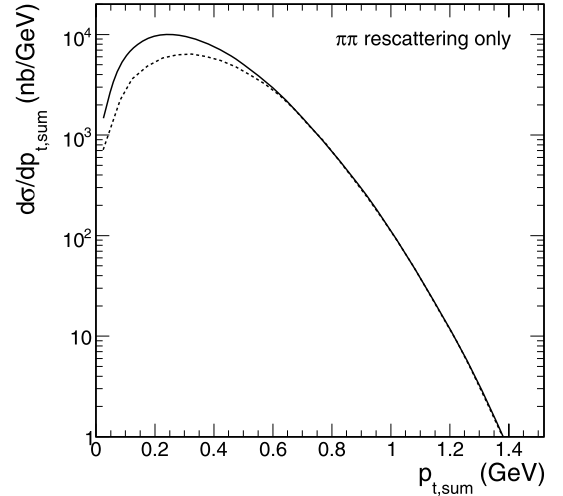


Fig. 8. Differential cross section $d\sigma/dp_{t,\text{sum}}$ for the $p\bar{p} \rightarrow p\bar{p}\pi^+\pi^-$ reaction at $\sqrt{s} = 5.5$ GeV. The solid line is the cross section without cuts, the dashed line includes cuts to remove regions of Roper resonance and double- Δ excitations.

take $\Delta M_{N^*} = 0.4$ GeV and $\Delta M_{\Delta} = 0.2$ GeV which are considerably bigger than the decay widths.

In Fig. 7 we present differential cross section $\frac{d^2\sigma}{dt_1 dt_2} = \frac{d\sigma}{dt_1} = \frac{d\sigma}{dt_2}$ (integrated over all other variables) for pion-pion rescattering only. The shape of the distribution reflects tensorial structure of the πNN vertices (see Eq. (2.1)) as well as t_1 or t_2 dependence of vertex form factor (see Eq. (2.2)). This plot illustrates how virtual are “initial” pions. In principle, measuring such distributions would allow to limit, or even extract, the πNN form factor in relatively broad range of t_1 or t_2 . This is not possible in elastic nucleon-nucleon scattering where many different exchange processes contribute.

In Fig. 8 we show differential cross section $d\sigma/dp_{t,\text{sum}}$, where $\vec{p}_{t,\text{sum}} = \vec{p}_{3t}(\pi^+) + \vec{p}_{4t}(\pi^-)$. For collinear (parallel to the parent nucleons) initial pions this distribution would be proportional to the Dirac $\delta(p_{t,\text{sum}})$. The deviation from $\delta(p_{t,\text{sum}})$ is therefore a measure of noncollinearity and is strongly related to virtualities of “initial” pions (see Fig. 7).

The two-pion invariant mass distribution given by the differential cross section $d\sigma/dM_{\pi\pi}$ is particularly interesting. Here (see Fig. 9) one can see two characteristic bumps corresponding to the

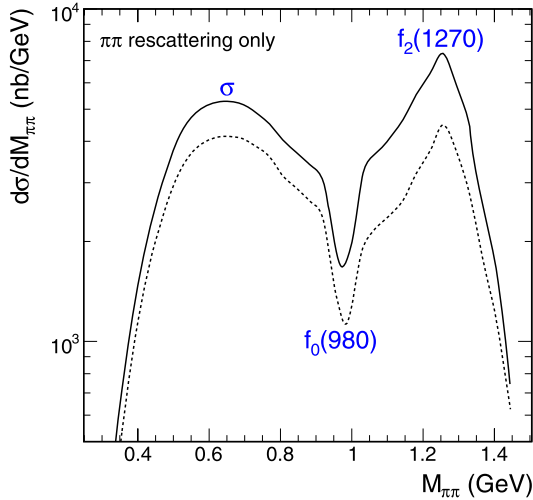


Fig. 9. Differential cross section $d\sigma/dM_{\pi\pi}$ for the $p\bar{p} \rightarrow p\bar{p}\pi^+\pi^-$ reaction at $\sqrt{s} = 5.5$ GeV. The solid line is the cross section without cuts, the dashed line includes cuts to remove regions of Roper resonance and double- Δ excitations.

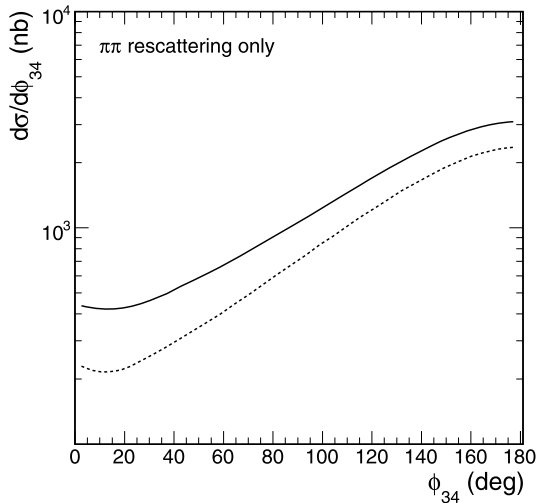


Fig. 10. Differential cross section $d\sigma/d\phi_{34}$ for the $p\bar{p} \rightarrow p\bar{p}\pi^+\pi^-$ reaction at $\sqrt{s} = 5.5$ GeV. The solid line is the cross section without cuts, the dashed line includes cuts to remove regions of Roper resonance and double- Δ excitations.

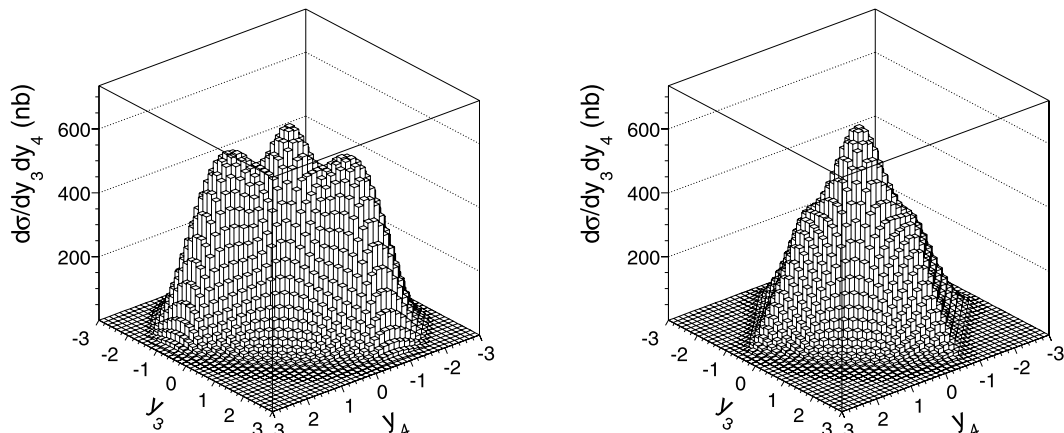


Fig. 11. Two-dimensional differential cross section $d\sigma/dy_3 dy_4$ in $y_3(\pi^+) \times y_4(\pi^-)$ for the $p\bar{p} \rightarrow p\bar{p}\pi^+\pi^-$ reaction at $\sqrt{s} = 5.5$ GeV (left panel). In the right panel we have included in addition cuts to remove regions of Roper resonance and double- Δ excitations.

famous scalar-isoscalar σ meson and tensor-isoscalar $f_2(1270)$ meson as well as the dip from $f_0(980)$. The cuts to remove regions of Roper resonance and double- Δ excitation only slightly modify the spectral shape.

The PANDA detector is supposed to be a 4π solid angle detector with good particle identification for charged particles and photons. This opens a possibility to study several correlation observables for outgoing particles. One of them is azimuthal angle correlation between charged outgoing pions ϕ_{34} , never discussed in the literature. In Fig. 10 we present differential cross section $d\sigma/d\phi_{34}$. Clearly a preference of back-to-back emissions can be seen. Imposing cuts on the Roper resonance and double- Δ excitation lowers the cross section but only mildly modifies the shape. Because the shape of the azimuthal angle correlations strongly depends on the reaction mechanism, measuring such correlation would provide then very valuable information.

In Fig. 11 we show differential cross section $d\sigma/dy_3 dy_4$ in the two-dimensional space (y_3, y_4) . For comparison in the right panel we show a similar distribution when extra cuts to remove regions of Roper resonance and double- Δ excitation are imposed. The cuts do not much affect the region of $y_3, y_4 \approx 0$. In practice, the cuts on the Roper resonance act for $(y_3 < 0$ and $y_4 < 0$) or $(y_3 > 0$ and $y_4 > 0)$, i.e. in the region where the two-pion rescattering contribution is small. The cuts on double- Δ excitation act for $(y_3 < 0$ and $y_4 > 0)$ or $(y_3 > 0$ and $y_4 < 0)$, i.e. in the region where the two-pion rescattering contribution is sizeable. This shows that the double- Δ excitation is more critical than the Roper resonance excitation in the context of extracting the pion-pion rescattering contribution.

5. Conclusions

We have calculated both differential and total cross sections for the $pp \rightarrow pp\pi^+\pi^-$ and $p\bar{p} \rightarrow p\bar{p}\pi^+\pi^-$ reactions close to threshold and for future PANDA experiments. Our results have been compared with very close to threshold data measured by the WASA Collaboration. We have shown that very close to threshold the pion-pion rescattering mechanism gives much smaller contribution than the excitation of the Roper resonance and its subsequent decay as well as the double- Δ excitation and subsequent decays studied in the past [1]. At low energies all these mechanisms overlap and it is not possible to extract the pion-pion rescattering contributions and therefore not possible to study the $\pi^0\pi^0 \rightarrow \pi^+\pi^-$ process.

Going to higher energies allows to find regions of the final state phase space where the pion–pion rescattering process dominates over the Roper resonance and double- Δ excitation mechanisms. Experiments at highest energies of the HESR (FAIR project) at GSI Darmstadt open a possibility to study the pion rescattering process and provide an excellent place for studying properties of the Roper $N^*(1440)$ resonance. At present it is not clear how precisely the pion rescattering can be studied experimentally as the PANDA detector is in the exploratory phase and its detailed final design is still an open issue. We expect that the minimal scenario would be to verify models like the one discussed in the present Letter. Whether the phase shift analysis is possible requires extra Monte Carlo studies including efficiencies of the PANDA detector. We hope that the cross section for exclusive production and the line shape (position and width) of the Roper resonance can be studied with the PANDA detector. GSI is only possible place where the exclusive $p\bar{p} \rightarrow p\bar{p}\pi^+\pi^-$ reaction can be studied at sufficiently large energy. At the Tevatron the pion rescattering cross section is completely negligible and other mechanisms becoming important [17].

We have presented several distributions which could be measured in the future with the PANDA detector at the GSI HESR. Particularly interesting is the distribution in two-pion invariant mass, where one should observe bumps related to the famous scalar-isoscalar σ -meson and to tensor-isoscalar $f_2(1270)$ meson as well as a dip from the interference with $f_0(980)$ and σ . This distribution is slightly different compared to the dependence of the total $\pi^0\pi^0 \rightarrow \pi^+\pi^-$ cross section on $M_{\pi\pi}$. This is caused mainly by the four-body phase space modifications.

The pions from the pion–pion rescattering are produced preferentially in opposite hemispheres, i.e. if one pion is produced at positive center-of-mass rapidities the second pion is produced at negative ones. This is similar to the double- Δ excitation mechanism. Imposing cuts on double- Δ excitation leaves untouched the region of midrapidities. Also the region of large $p_{t,\text{sum}}$ stays unmodified by the cuts on double- Δ excitations.

Acknowledgements

Discussions and communications with Benoit Loiseau are acknowledged. This work was partially supported by the Polish Min-

istry of Science and Higher Education (MNiSW) under Contract MNiSW N N202 249235.

References

- [1] L. Alvarez-Ruso, E. Oset, E. Hernandez, Nucl. Phys. A 633 (1998) 519.
- [2] C. Amsler, et al., Particle Data Group, Phys. Lett. B 667 (2008) 1.
- [3] B. Ananthanarayan, G. Colangelo, J. Gasser, H. Leutwyler, Phys. Rep. 353 (2001) 207.
- [4] G. Colangelo, J. Gasser, H. Leutwyler, Nucl. Phys. B 603 (2001) 125.
- [5] S. Descotes-Genon, N.H. Fuchs, L. Girlanda, J. Stern, Eur. Phys. J. C 24 (2002) 469.
- [6] I. Caprini, G. Colangelo, H. Leutwyler, Phys. Rev. Lett. 96 (2006) 132001.
- [7] J.R. Pelaez, F.J. Yndurain, Phys. Rev. D 71 (2005) 074016.
- [8] R. Kamiński, J.R. Pelaez, F.J. Yndurain, Phys. Rev. D 77 (2008) 054015.
- [9] R. Kamiński, R. Garcia-Martin, P. Gryniewicz, J.R. Pelaez, Nucl. Phys. B 186 (2009) 318; R. Garcia-Martin, R. Kamiński, J.R. Pelaez, Int. J. Mod. Phys. A 24 (2009) 590.
- [10] R. Kamiński, L. Lesniak, B. Loiseau, Phys. Lett. B 551 (2003) 241.
- [11] T.E.O. Ericson, B. Loiseau, A.W. Thomas, Phys. Rev. C 66 (2002) 014005, arXiv: hep-ph/0009312v2.
- [12] R. Machleidt, K. Holinde, Ch. Elster, Phys. Rep. 149 (1987) 1; D.V. Bugg, R. Machleidt, Phys. Rev. C 52 (1995) 1203.
- [13] A. Szczurek, J. Speth, Nucl. Phys. A 555 (1993) 249; B.C. Pearce, J. Speth, A. Szczurek, Phys. Rep. 242 (1994) 193; J. Speth, A.W. Thomas, Adv. Nucl. Phys. 24 (1997) 83.
- [14] Z. Ouyang, J.-J. Xie, B.-S. Zou, H.-S. Xu, Nucl. Phys. A 821 (2009) 220, arXiv: 0808.3257v3 [nucl-th].
- [15] H. Clement, et al., PROMICE/WASA Collaboration, Contributed to Conference on Quarks and Nuclear Physics (QNP 2002), Jülich, Germany, 9–14 June 2002, arXiv:nucl-ex/0210006v1.
- [16] S. Hirenzaki, P. Fernández de Córdoba, E. Oset, Phys. Rev. C 53 (1996) 277.
- [17] P. Lebiedowicz, A. Szczurek, in preparation.
- [18] D.V. Bugg, et al., Phys. Rev. B 133 (1964) 1017.
- [19] D.R.F. Cochran, et al., Phys. Rev. D 6 (1972) 3085.
- [20] L.G. Dakhno, et al., Sov. J. Nucl. Phys. 37 (1983) 540.
- [21] F. Shimizu, et al., Nucl. Phys. A 386 (1982) 571.
- [22] F.H. Cverna, et al., Phys. Rev. C 23 (1981) 1698.
- [23] J. Pätzold, PhD thesis, Univ. Tübingen (2002), <http://w210.ub.uni-tuebingen.de/dbt/volltexte/2002/550>; J. Pätzold, et al., PROMICE/WASA Collaboration, Phys. Rev. C 67 (2003) 052202.
- [24] W. Brodowski, et al., PROMICE/WASA Collaboration, Phys. Rev. Lett. 88 (2002) 192301.
- [25] J. Johanson, et al., PROMICE/WASA Collaboration, Nucl. Phys. A 712 (2002) 75.
- [26] S. Abd El-Bary, et al., COSY-TOF Collaboration, Eur. Phys. J. A 37 (2008) 267, arXiv:0806.3870v1 [nucl-ex].
- [27] A. Buzzo, et al., JETSET Collaboration, Z. Phys. C 76 (1997) 475.